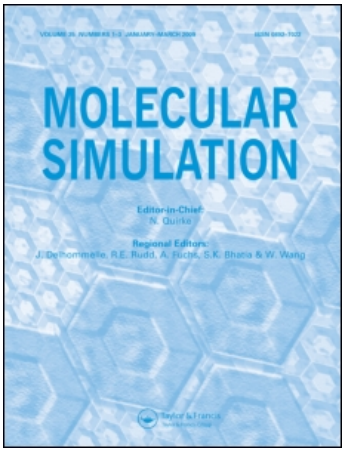

Molecular Simulation
Publication details, including instructions for authors and subscription information:
http://www.informaworld.com/smpp/title~content=t713644482

Computer Simulation Studies of Zeolite Structure

R. A. Jackson[a]; C. R. A. Catlow[a]
[a] Department of Chemistry, University of Keele, Staffs, UK

To cite this Article Jackson, R. A. and Catlow, C. R. A.(1988) 'Computer Simulation Studies of Zeolite Structure', Molecular Simulation, 1: 4, 207 — 224
To link to this Article: DOI: 10.1080/08927028808080944
URL: http://dx.doi.org/10.1080/08927028808080944

Molecular Simulation, 1988, Vol. 1, pp. 207–224
Photocopying permitted by license only
Reprints available directly from the publisher

COMPUTER SIMULATION STUDIES OF ZEOLITE STRUCTURE

R.A. JACKSON and C.R.A. CATLOW

Department of Chemistry, University of Keele, Keele, Staffs. ST5 5BG, UK

(*Received April, 1987, in final form August, 1987*)

This paper describes the use of lattice energy minimization to obtain structural information on zeolites. Examples are given of the use of this technique in the study of non-framework cation distributions, and in energy minimization of complete structures. The zeolites faujasite, zeolite A and silicalite are considered.

KEY WORDS: Energy minimization, potentials, zeolites, zeolite A, faujasite, silicalite

1. INTRODUCTION

Zeolites are porous framework structured aluminosilicates (in some cases pure silica polymorphs). They have attracted considerable attention in recent years owing to

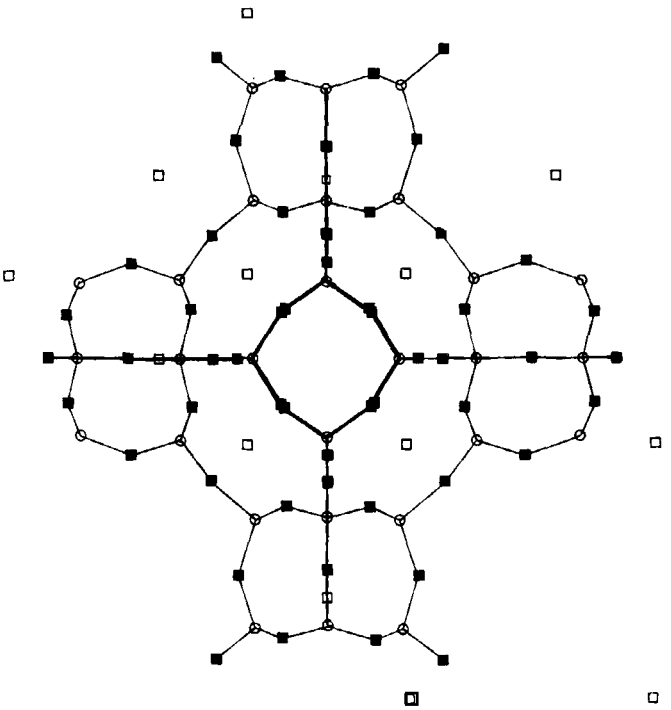

Figure 1 Zeolite A, showing the sodalite unit. (See colour plate I.)

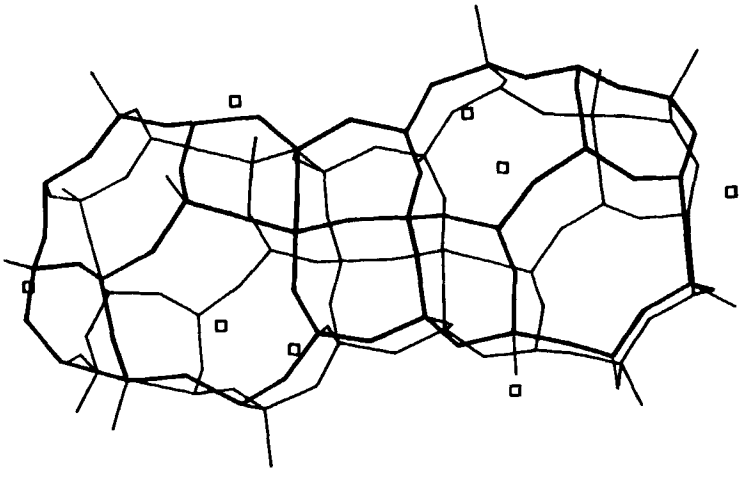

Figure 2 Faujasite, showing positions of the S_{II} cations.

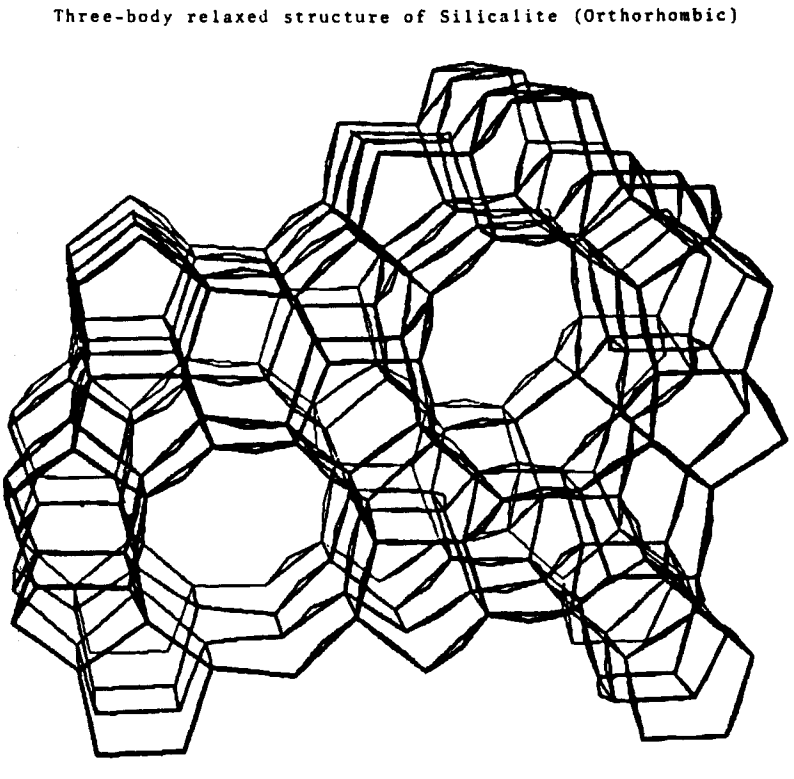

Figure 3 Silicalite 3-d structure (orthorhombic).

their use as shape-selective catalysts [1]. A more traditional use arises from their ion exchange properties; the substitution of Al for Si in the framework requires charge compensation by extra-framework cations (or protons) that are relatively loosely bound and readily exchanged.

The structures of many zeolites are based on cubo-octahedral "sodalite cages", which may be fused together to give the sodalite structure, joined across the 4-rings to give zeolite A (Figure 1) or joined across the 6-rings to give faujasite (Figure 2). Other modes of linkage [2] yield a variety of structures. A different set of structures are based on 5-rings, some of which are known by their generic name "pentasils". The most celebrated of these materials is ZSM-5 and the closely-related silicalite (Figure 3), which have potentially valuable catalytic properties in the synthesis of gasolene from methanol.

Computer simulation studies are playing an increasing role in several aspects of zeolite chemistry. The calculations can be used to predict (i) framework structures and stabilities, (ii) the position of extra-framework cations, (iii) the location of sorbed molecules and (iv) reaction pathways of sorbed molecules using quantum mechanical methods. The present paper will concentrate on the first two areas. These are certainly the most basic aspects and, as will be seen, their study demands that careful attention be paid to the methodology of the calculations and to the choice of interatomic potentials. Having discussed both these points, an account is given of recent applications to faujasite, zeolite A and silicalite. The paper concludes with a summary of the present status of the field, and of the likely directions of future developments.

2. LATTICE ENERGY MINIMIZATION

The technique of lattice energy minimization is used in these calculations. It enables structures corresponding to minimum lattice energies to be calculated. This may be done in two ways: either the atomic positions only are adjusted until the minimum is obtained (constant volume minimization) or, additionally, the unit cell parameters are adjusted to remove any remaining strains in the lattice (constant pressure minimization). In the case of zeolites, whole structures may be minimized or, alternatively, the framework may be held rigid and only the non-framework cations relaxed to equilibrium. This latter approach was adopted for faujasite (see section 4).

Two types of energy minimization technique have been used in zeolite simulations. The first method, the Newton–Raphson technique [3] requires calculations of the matrix of second derivatives of the potential with respect to atomic displacements, and subsequent inversion of this matrix. In some of the earlier calculations on silicalite [4], this calculation was too large for the available computer memory (on the CRAY 1S), so an alternative minimization method had to be employed. This method, the Conjugate Gradients technique [5] requires that only the first derivatives of the potential with respect to atomic displacements be calculated, and it is thus less expensive in terms of computer memory requirements. It is, however, less efficient, being slower by up to an order of magnitude.

Finally, the same techniques adopted for lattice energy minimization are currently being applied to the problem of calculating minimum free energies [6]. This important new development will be discussed in a future publication. In concluding this section it should be noted that the techniques summarized above are quite standard (see e.g. reference 7). In applying them to zeolites the most important question concerns interatomic potentials, which are discussed in the next section.

3. POTENTIALS

The specifications of interatomic potentials is of central importance in any computer simulation study. In carrying out calculations on zeolites, use has been made of a potential model that has been very successful in calculating the structural and defect properties of a wide range of ionic and semi-ionic solids [7]. The basic form for the potential describing the interaction of a pair of ions is given below:

$$V(r_{ij}) = q_i q_j / r_{ij} + A_{ij} \exp(-r_{ij}/\varrho_{ij}) - C_{ij}/r_{ij}^6$$

Here, i and j refer to the interacting ions, q_i and q_j to their charges, and A_{ij}, ϱ_{ij} and C_{ij} are short-range potential parameters.

In most potentials, formal charges have been used (lattice energy sums are treated in detail in an appendix). Ionic polarizability can be incorporated by using the shell model [8] in which an ion is represented by a core and a shell joined by a harmonic spring; the sum of core and shell charges is the formal charge. In the calculations reported in this paper, the shell model has been used in some cases, but only for oxygen ions.

Short-range potential parameters may be obtained by two main methods. The first of these, the empirical method, involves fitting a potential to crystal properties, such as structural data, dielectric and elastic constants. The potentials used to describe the zeolite framework in this study were all determined empirically. The second method

Table 1 Potential parameters for zeolite frameworks.

(a) 2-body model (fixed framework)

Interaction	*A(eV)*	*ϱ(Å)*	*C(eVÅ⁶)*
$Si^{4+} \ldots O^{2-}$	998.98	0.3455	0.0
$Al^{3+} \ldots O^{2-}$	1460.3	0.29912	0.0
$O^{2-} \ldots O^{2-}$	22764.0	0.149	27.88

(b) 3-body model, rigid ions

Interaction	*A(eV)*	*ϱ(Å)*	*C(eVÅ⁶)*
$Si^{4+} \ldots O^{2-}$	1584.167	0.32962	52.64511
$Al^{3+} \ldots O^{2-}$	1460.3	0.29912	0.0
$O^{2-} \ldots O^{2-}$	22764.0	0.149	27.88

3-body potential for Si^{4+}, Al^{3+}: $k = 4.5815\,\text{eV rad}^{-2}$
$\theta_0 = 109.47°$

(c) 3-body model, shell model

Interaction	*A(eV)*	*ϱ(eV)*	*C(eVÅ⁶)*
$Si^{4+} \ldots O^{2-}$	1283.907	0.32052	10.66158
$Al^{3+} \ldots O^{2-}$	1460.3	0.29912	0.0
$O^{2-} \ldots O^{2-}$	22764.0	0.149	27.88

Harmonic potential for O^{2-}: $Y^- = -2.86902\,|e|$, $k = 74.92\,\text{eVÅ}^{-2}$
3-body potential for Si^{4+}, Al^{3+}: $k = 2.09724\,\text{eV rad}^{-2}$
$\theta_0 = 109.47°$

(d) Alternative 3-body potential for $Al^{3+} \ldots O^{2-}$

A(eV)	*ϱ(Å)*	*C(eVÅ⁶)*
498.602	0.38528	0.0

3-body potential: $k = 2.0705\,\text{eV rad}^{-2}$ $\theta_0 = 109.47°$

Table 2 Potential parameters for non-framework cations.

Interaction	*A(eV)*	*ϱ(Å)*	*C(eVÅ⁶)*
$K^+ \ldots O^{2-}$	1000.30	0.36198	10.569
$Sr^{2+} \ldots O^{2-}$	1952.39	0.33685	19.22
$Na^+ \ldots O^{2-}(1)$	1226.84	0.3065	0.0
$Na^+ \ldots O^{2-}(2)$	5836.84	0.2387	0.0

For all short-range potentials a cutoff of ~ 10 Å was used.

of calculating potential parameters is to make use of an appropriate theoretical technique, in this case the "electron gas" method [9] used to calculate parameters for the non-framework cation . . . framework interactions.

Finally, in order to be able to simulate framework relaxation in zeolites it is necessary to include an extra term in the potential to take account of the directionality of the bonding of oxygen ions with silicon or aluminium ions. This term, which is defined for each O–Si–O or O–Al–O bond, takes the form

$$V_{3\text{-}body} = 1/2\ k(\theta - \theta_0)^2$$

In this equation, k is the bond force constant and θ_0 is the equilibrium bond angle.

In most of the calculations reported, all bonds were defined using a parameterization of the above potential form to α-quartz. However, in one calculation on Na^+ zeolite *A* a separately fitted potential was used to describe bonding about aluminium ions.

All potentials used are tabulated (Tables 1 and 2) and, in the following sections of the paper where examples are given of specific calculations, reference is made to the potential used and the appropriate table.

4. FAUJASITE

As mentioned in the Introduction, the zeolite faujasite is made up of sodalite units joined through the 6-rings (Figure 2). If the Si/Al ratio is in the range 1–1.5, it is known as zeolite X; if the Si/Al ratio is in the range 1.5–3 it is known as zeolite Y.

Calculations on faujasite were reported by Sanders and Catlow [10]. These had the limited aim of predicting and rationalizing the cation distribution in this zeolite. The work concentrated on K^+ faujasite with a Si/Al ratio of 1.4 (i.e. a zeolite X) and explored the effects on the cation distribution of changes in the distribution of the framework tetrahedral sites.

As shown in Figure 4, three sites have been identified for cations in faujasite. The S_I site is within the hexagonal prisms that link the cuboctahedra; the S_I' is adjacent to the linking hexagons but within the sodalite cage. The S_{II} site is at the centre of the 6-rings that project outwards into the supercage.

The simulation reported by Sanders [11] and by Sanders and Catlow [10] first showed, by straightforward Madelung energy calculations, that the S_{II} site is by the most energetically favoured. This is apparent from the Madelung energies reported in Table 3. It is, moreover, consistent with the observed full occupany of these sites determined in a crystallographic study [12] on zeolite X. The more intriguing question concerns the distribution of the remaining cations over the S_I and S_I' sites. Sanders [11] undertook a comprehensive study of this problem in which all permutations of cations over these sites were examined; for the more favoured distributions, the energy was

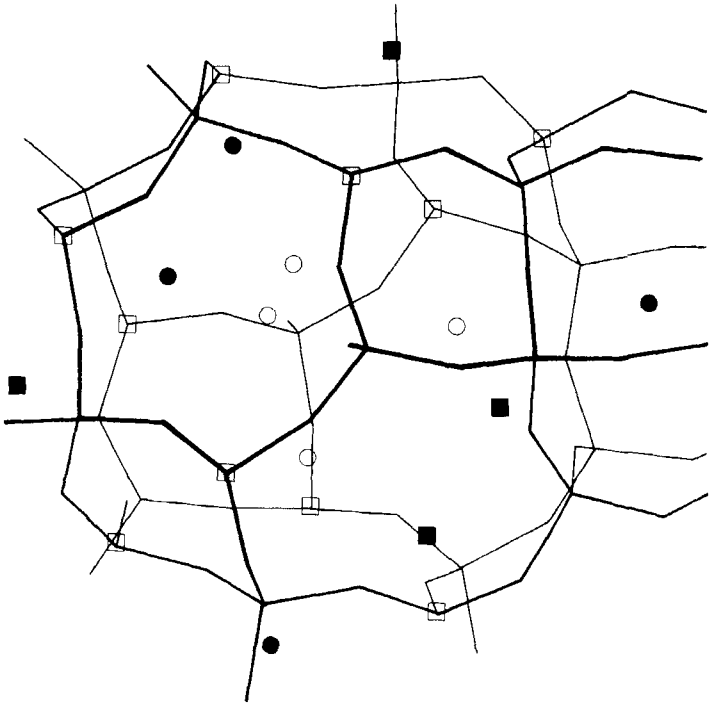

Figure 4 Cation positions in faujasite S_I . . . ●, S_I' . . . ○, S_{II} . . . ■. (See colour plate II.)

then minimized with respect to the cation coordinate. The results are summarized in Table 4, and the most significant findings are as follows:

1. The most energetically favourable cation distribution has equal occupation of S_I and S_I' sites. This result is in agreement with the results of crystallographic studies [12].
2. For certain Al distributions, occupancy of adjacent S_I and S_I' sites is predicted on energetic grounds. Favourable cation–framework interactions are sufficient to outweigh the unfavourable cation–cation repulsions.
3. The energies of structures with different Al distributions are very similar. It seems that readjustment of the cations can largely smooth out the effects of changes in the Si/Al distribution over the framework sites.
4. The energy minimized cation sites are reasonably close (within 0.2 Å) of the crystallographically determined sites.

It is clear therefore from this study that energy minimization techniques provide a straightforward and computationally inexpensive way of studying the cation distributions in zeolites, and that useful information can be obtained by calculations that vary only the non-framework cation positions. The potentials used in this study are given in Tables 1(a) and 2.

Table 3 Madelung energies of cation sites in faujasite (eV).

Cation coordinate			*Structures*							
S_I										
0.0	0.0	0.0	−9.163	−6.747	−7.955	+4.317	−9.246	−7.955	−1.215	−7.997
0.25	0.25	0.25	−1.215	−9.163	−2.423	−9.163	−1.215	−2.423	−8.580	−2.381
0.0	0.25	0.25	−9.163	−2.465	−7.955	−7.913	−7.913	−7.955	−5.189	−7.997
0.25	0.0	0.25	−1.215	−2.381	−7.997	−7.997	−2.381	−2.423	−5.772	−2.381
S_I'										
0.076	0.076	0.076	−3.345	−1.446	−2.147	+3.490	−3.563	−2.147	+1.022	−2.505
0.076	0.174	0.174	−3.345	−0.037	−2.147	−2.286	−2.286	−2.147	−0.495	−2.505
0.174	0.076	0.174	+1.022	+0.182	−0.175	−2.505	+0.182	−0.175	−2.598	+0.108
0.174	0.174	0.076	+1.022	−3.345	−0.175	−3.345	+1.022	−0.175	−2.575	+0.108
−0.076	−0.076	−0.076	−3.345	−1.446	−2.643	+3.490	−3.563	−2.643	+1.022	−2.505
−0.076	−0.174	−0.174	−3.345	−0.037	−2.643	−2.286	−2.286	−2.643	−1.828	−2.505
−0.174	−0.076	−0.174	+1.022	+0.182	+0.320	−2.505	+0.182	+0.302	−0.565	+0.108
−0.174	−0.174	−0.076	+1.022	−3.345	+0.320	−3.345	+1.022	+0.302	−3.274	+0.108
S_{II}										
0.2473	0.2473	0.2473	−13.324	−15.531	−15.980	−17.074	−10.894	−15.980	−16.302	−13.190
0.2473	0.0027	0.0027	−13.324	−13.961	−15.980	−15.665	−15.665	−15.980	−16.036	−13.190
0.0027	0.2473	0.0027	−16.302	−16.437	−13.647	−13.190	−16.437	−13.647	−12.983	−16.437
0.0027	0.0027	0.2473	−16.302	−13.324	−13.647	−13.324	−16.302	−13.647	−13.932	−16.437
−0.2473	−0.2473	−0.2473	−13.324	−15.531	−12.875	−17.074	−10.894	−12.875	−16.302	−13.190
−0.2473	−0.0027	−0.0027	−13.324	−13.961	−12.875	−15.665	−15.665	−12.875	−13.591	−13.190
−0.0027	−0.2473	−0.0027	−16.302	−16.437	−16.751	−13.190	−16.437	−16.751	−16.778	−16.437
−0.0027	−0.0027	−0.2473	−16.302	−13.324	−16.751	−13.324	−16.302	−16.751	−12.582	−16.437

Table 4 Minimized lattice energy for faujasite.

Structures	*Lattice energy/eV*	*Minimized lattice energy/eV*
1	−5208.737	−5210.513
2	−5209.730	−5211.249
3	−5207.368	−5209.798
4	−5209.504	−5210.974
5	−5208.735	−5210.555
6	−5209.475	−5210.842
7A	−5209.522	−5210.964
7B	−5209.810	−5211.162
8A	−5206.052	−5207.476
8B	−5206.390	−5207.532

5. ZEOLITE A

In zeolite A, the sodalite units are joined through the 4-rings; Na^+ zeolite A is illustrated in Figure 1. In this paper, studies on two forms of zeolite A are described, the first, a study of Sr^{2+} zeolite A, and the second, a study of Na^+ zeolite A.

Sr^{2+} Zeolite A

Calculations on Sr^{2+} zeolite A were reported by Sanders, Catlow and Smith [13] and by Sanders [11]. The structure is illustrated in Figure 5. The first study [13] followed the same procedure as the work of Sanders and Catlow on faujasites [10] described in the previous sections, in that the zeolite framework was held fixed and the non-framework cation distribution varied. Two sites were considered for Sr^{2+} ion occupancy, both associated with the 6-rings, but one (type I) projecting into the supercage, and one (type 2) displaced into the sodalite unit. The calculations investigated the most stable distribution of 12 Sr^{2+} ions over sites (1) and (2), and examined a range of ratios of (1):(2) occupancy. Many possible cation distributions exist for each occupancy ratio, but only the likely ones without adjacent vacancies were considered. For each occupancy, the distribution with the lowest initial energy was taken, and energy minimized with respect to the cation positions. The minimum energies are reported in Table 5. Also in this table, the energies of the same distributions after displacement of a cation to a third site (3) are given; this third site is located near an 8-ring, and its existence had been a matter of debate from previous experimental studies [14, 15]. As can be seen from the table, it is energetically unfavourable to transfer a cation to this site, and this supports the findings of the second experimental study [15]. Figure 5 shows the most stable distribution of cations.

Sanders [11] reported an extension of this study to incorporate framework relaxations; i.e. the energy minimization was carried out with respect to the whole structure, and not just the non-framework cations. The two distributions with the lowest energy from the previous study were taken, and the lattice energy was minimized to constant volume, using the conjugate gradients method. The lattice energies obtained are also reported in Table 5. Good agreement with experiment was obtained when the calculated and experimental bond lengths and angles were compared; this is fully discussed in reference [11].

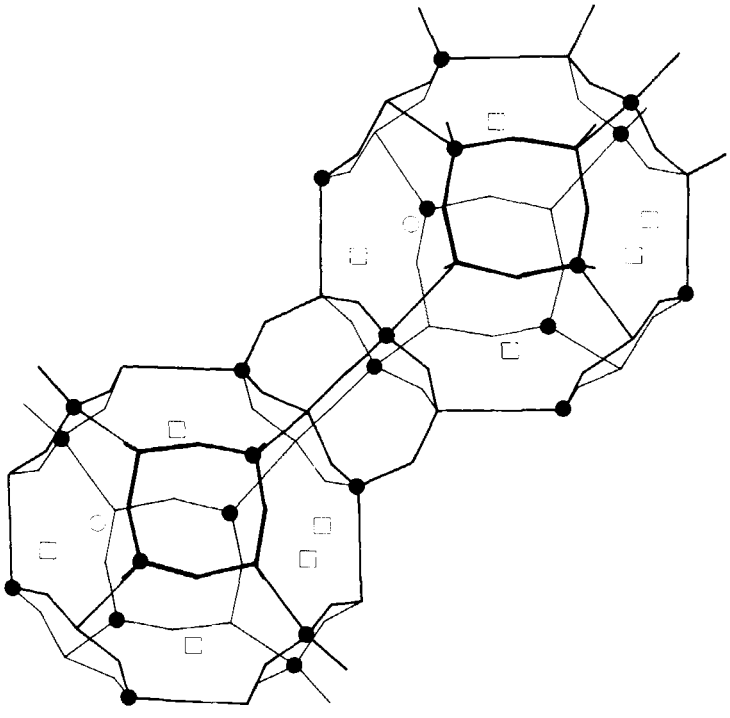

Figure 5 Sr^{2+} zeolite A, showing the most stable distribution of Sr^{2+} cations. Sr(1) . . . □, Sr(2) . . . ●. (See colour plate III.)

Na^+ Zeolite A

Na^+ zeolite A has been the subject of a recent detailed study with a view to establishing the accuracy with which lattice energy minimization can reproduce experimental data.

The structure was taken from an experimental study by Pluth and Smith [16] that employed single crystal X-ray diffraction. Three sites were found to be occupied by Na^+ ions, associated respectively with 8-, 6- and 4-rings. The occupancy of the 4-ring site was, however, found to be very low. The Si/Al ratio was 1:1.

In the simulation a unit cell was used in which all the available 6- and 8-ring sites were filled, but none of the 4-ring sites. The formula of the unit cell was

Table 5 Calculated lattice energies for Sr^{2+} zeolite A.

No of Sr atoms in site 1	*Lattice energies/eV*		
	Zero occupancy of site 3	*After removal of 1 Sr to site 3*	*After framework relaxation*
12	−5204.58	−5200.61	−5420.47
11	−5204.49	−5200.84	
10	−5204.61	−5200.28	−5420.50
9	−5204.46	−5200.48	
8	−5204.48	−5200.44	

Table 6 Calculated lattice energies for Na^+ zeolite A.

Model	*Lattice energies/eV*	
	After relaxation to constant volume	*After relaxation to constant pressure*
(a)	−5162.32	−5163.96
(b)	−5179.02	−5179.66
(c)	−5297.73	−5297.93
(d)	−5314.46	−5314.51
(e)	−5203.58	−5203.65

$Na_{22}Al_{24}Si_{24}O_{96}$. The charge imbalance was made up by a small decrease in the oxygen charge.

A range of potential models were used, as detailed below. All potential models were used, as detailed below. All potential parameters are tabulated in Table 3.

model (a) rigid ion O^{2-} + Na^+ . . . O^{2-} potential 1
model (b) rigid ion O^{2-} + Na^+ . . . O^{2-} potential 2
model (c) shell model O^{2-} + Na^+ . . . O^{2-} potential 1
model (d) shell model O^{2-} + Na^+ . . . O^{2-} potential 2
model (e) as (d) but with the alternative 3-body O–Al–O potential

The structure was then minimized to constant volume using each of the above potential models. Calculated lattice energies are given in Table 6. Bond lengths and bond angles obtained are compared with the experimental values in Tables 7–9.

From these tables, the following general observations can be made:

1. All potentials reproduce the experimental structure to broadly the same accuracy.
2. All potentials tend to underestimate slightly the Si–O bond lengths.
3. The most difficult angles to reproduce are those involving two tetrahedral atoms and a bridging oxygen atom. However, the most detailed model, model (e), reproduces these angles reasonably well.
4. The worst agreement in bond lengths concerns the Na(2) atoms located in the 8-rings. The main reason for this is that each 8-ring has four possible positions for occupation by Na^+ ions, and in the calculation a definite choice had to be made which might not correspond to the experiment.
5. All potentials used were obtained by fitting to other structures (usually α-quartz), except the Na^+ . . . O^2 potentials, which were calculated by the electron gas method. It is gratifying that such good overall agreement was obtained for a material other than that used to fit the potentials. However, to improve the

Table 7 Comparison of experimental and calculated Si–O bonds and O–Si–O angles.

Bond length or angle	*Experiment [16]*	*Model (a)*	*Model (b)*	*Model (c)*	*Model (d)*	*Model (e)*
Si–O(1)	1.595	1.537	1.493	1.525	1.523	1.531
Si–O(2)	1.586	1.541	1.562	1.551	1.554	1.562
Si O(3)	1.604	1.579	1.602	1.548	1.550	1.554
Mean	1.597	1.552	1.552	1.541	1.542	1.549
O(1)–Si–O(2)	108.8	109.5	110.4	107.7	106.3	106.2
O(1)–Si–O(3)	111.3	109.3	109.7	110.0	110.9	110.9
O(2)–Si–O(3)	107.2	109.2	108.3	108.7	107.9	107.7

Table 8 Comparison of experimental and calculated Al–O bonds and O–Al–O angles.

Bond length or angle	*Experiment [16]*	*Model (a)*	*Model (b)*	*Model (c)*	*Model (d)*	*Model (e)*
Al–O(1)	1.723	1.731	1.734	1.740	1.747	1.718
Al O(2)	1.717	1.718	1.721	1.761	1.761	1.747
Al O(3)	1.741	1.736	1.739	1.777	1.784	1.806
Mean	1.731	1.728	1.731	1.759	1.764	1.757
O(1)–Al–O(2)	108.1	109.5	107.1	114.1	117.0	118.0
O(1)–Al–O(3)	112.3	108.8	109.9	108.4	108.2	108.4
O(2)–Al–O(3)	106.0	109.7	109.7	107.4	105.6	105.2

Table 9 Comparison of experimental and calculated Na . . . O distances and T–O–T angles.

Bond length or angle	*Experiment [16]*	*Model (a)*	*Model (b)*	*Model (c)*	*Model (d)*	*Model (e)*
T–O(1)–T	142.2	142.4	152.1	137.1	141.3	142.2
T–O(2)–T	164.7	169.7	159.8	171.6	165.4	165.1
T–O(3)–T	144.8	153.3	148.3	151.0	147.5	144.6
Na(1)–3O(3)	2.3227	2.4707	2.3596	2.4768	2.3735	2.3776
Na(1)–3O(2)	2.9146	2.8995	2.9407	2.9672	2.9911	2.9926
Na(2)–O(1)	2.557	2.6643	2.3832	2.7069	2.5181	2.5115
Na(2)–O(1)	2.673	2.8116	2.4332	2.8307	2.4043	2.3985

agreement (especially for the Si–O bonds lengths) some refitting of the potentials may be needed.

6. SILICALITE

Silicalite (Figure 3) is a member of the family of "pentasil" zeolites. It is the siliceous analogue of ZSM-5, which has important catalytic properties. Hope [4] applied constant volume lattice energy minimization to the experimentally determined orthorhombic structure [17], using the conjugate gradients technique. More recently, with the availability of the CRAY X-MP/48 supercomputer, the structure has been minimized using the Newton–Raphson method. Minimizations to constant volume and to constant pressure have been carried out.

Minimized lattice energies are given in Table 10. These were obtained using the rigid ion 3-body potentials given in Table 1(b). Displacements of the silicon atoms were all less than 0.1 Å; most oxygen atom displacements were less than 0.2 Å. A later study will analyse bond lengths and angles in a similar way to that adopted for Na^+ zeolite A in this paper. As a result of the minimization to constant pressure, no departure from orthorhombic symmetry was observed.

Table 10 Calculated lattice energies for silicalite.

Form of energy minimization	*Lattice energies/eV*	
	Constant volume	*Constant pressure*
Conjugate gradients	−11884.462	–
Newton–Raphson unit cell: $Si_{96}O_{192}$	−11885.673	−11893.8667

7. CONCLUSION

This paper has shown that lattice energy minimization can be used to obtain useful structural information on zeolites. The technique has been applied to studying details of non-framework cation distribution, and to calculating minimum energy configurations for structures. The agreement with experiment obtained in this latter application is generally good, and with minor modifications it will be possible to calculate highly accurate structural properties for zeolites. The ability to perform such calculations will be of great value in crystallographic analysis and in studies of stability of new zeolite compounds.

Acknowledgements

The authors are grateful to J.V. Smith, J.M. Thomas, P. Barnes, M. Leslie, S.C. Parker, R. van Santen and G. Ooms for useful discussions. R.A.J. would like to thank Shell Research BV, Amsterdam, for financial support.

APPENDIX

The methods for evaluating lattice sums are now described, following the approach of Catlow and Norgett [18]. To evaluate the lattice energy per unit cell, we must transform the slowly converging Madelung sums in the potential (see section 3) into forms that may be rapidly computed. The Ewald transformation expresses the Coulomb sums as rapidly converging series. The physical basis of the method, as clearly described by Tosi [19], is the replacement of each point charge by a Gaussian charge distribution at the appropriate lattice site. This gives a more smoothly varying overall charge distribution. The Coulomb potential may be evaluated from the Fourier transform of this charge density. The charge is periodic in the lattice so that the transform involves contributions only from reciprocal lattice vectors. The sum over such vectors converges rapidly because the charge distribution has been smoothed. The second term is the difference in potential of the point-charge and substitute Gaussian-charge distributions. These latter contributions are equal except for lattice sites in the immediate vicinity of the point where the potential is evaluated.

Mathematically, the transformation of the Coulomb series is best effected by a direct but less transparent series of manipulations. We first write

$$\frac{1}{r} = \frac{2}{\pi^{1/2}} \int_0^\infty \exp(-r^2t^2)dt \tag{A.1}$$

and evaluate the integral separately between 0 and η and η and ∞. The value chosen for η determines the efficiency of the method and we determine the most effective value at the end of the appendix. In the upper range

$$\frac{2}{\pi^{1/2}} \int_\eta^\infty \exp(-r^2t^2)dt = \frac{2}{\pi^{1/2}r} \int_{\eta r}^\infty \exp(-s^2)ds = 1/r \operatorname{erfc}(\eta r) \tag{A.2}$$

For large η, $\operatorname{erfc}(\eta r)$ is a rapidly decreasing function of r and $\operatorname{erfc}(\eta r)$ is effectively a short-range potential in the direct lattice. We subsequently combine it with the explicit short-range interaction but only after considering the remainder of the integral in Equation (A.1).

In the lower range, the integral is Fourier transformed:

$$\frac{2}{\pi^{1/2}}\int_0^{\eta}\exp(-r^2t^2)dt = \frac{2}{\pi^{1/2}}\int_0^{\eta}dt\left(\frac{1}{2t\pi^{1/2}}\right)^3\int_{-\infty}^{\infty}\mathrm{d}^3\mathbf{K}\exp(-K^2/4t^2)\exp(-i\mathbf{K}.\mathbf{r}),$$

where

$$K^2 = |\mathbf{K}|^2. \tag{A.3}$$

With a variable change $s = -K^2/4t^2$ so that $ds = K^2dt/2t^3$, the first integral may be evaluated so that

$$\frac{2}{\pi^{1/2}}\int_0^{\eta}\exp(-r^2t^2)dt = \frac{1}{2\pi^2}\int_{-\infty}^{\infty}d^3\mathbf{K}\frac{\exp(-K^2/4\eta^2)}{K^2}\exp(-i\mathbf{K}.\mathbf{r}). \tag{A.4}$$

We then replace the integral $\int_{-\infty}^{\infty}d^3\mathbf{K}$ by a summation over **K** vectors defined so that

$$\mathbf{K} = 2\pi(n_1\mathbf{k}_1 + n_2\mathbf{k}_2 + n_3\mathbf{k}_3),$$

where $n_1n_2n_3$ are integers. $\mathbf{k}_1$, $\mathbf{k}_2$ and $\mathbf{k}_3$ satisfy the relation $\mathbf{k}_i.\mathbf{a}_j = \delta_{ij}/N^{1/3}$ where $\mathbf{a}_i$ is a fundamental lattice vector, δ_{ij} is one if $i = j$ but otherwise zero and N is the number of unit cells in the crystal. The volume per **K** vector is $(2\pi)^3\mathbf{k}_1.(\mathbf{k}_2 \times \mathbf{k}_3)$ which is $(2\pi)^3/Nv_c$ with v_c the volume of the unit cell. This follows because the **K** vectors are reciprocal lattice vectors divided by $N^{1/3}$ and the reciprocal cell volume is $1/v_c$. Then substituting $(2\pi)^3/Nv_c\sum_{\mathbf{K}}$ for $\int_{-\infty}^{\infty}$ in Equation (A.4) gives

$$\frac{2}{\pi^{1/2}}\int_0^{\eta}\exp(-r^2t^2)dt = \frac{4\pi}{Nv_c}\sum_{\mathbf{K}}\frac{\exp(-K^2/4\eta^2)}{K^2}\exp(-i\mathbf{K}.\mathbf{r}). \tag{A.5}$$

The Coulomb part of the lattice energy may now be written, using Equations (A.2) and (A.5), as

$$\begin{aligned}&\frac{1}{2}\sum_{nn'l}{}'\left(\frac{1}{2}\right)\frac{4\pi}{Nv_c}\sum_{\mathbf{K}}\frac{\exp(-K^2/4\eta^2)}{K^2}\sum_{nn'l}{}'q_nq_{n'}\exp(-i\mathbf{K}.\mathbf{r}_{nn'l}) + \frac{1}{2}\sum_{nn'l}{}'q_nq_{n'}\frac{\mathrm{erfc}(\eta r_{nn'l})}{r_{nn'l}}\\ &= \left(\frac{1}{2}\right)\frac{4\pi}{Nv_c}\sum_{\mathbf{K}}\frac{\exp(-K^2/4\eta^2)}{K^2}\sum_{nn'}{}'q_nq_{n'}\exp(-i\mathbf{K}.\{\mathbf{r}_n - \mathbf{r}_{n'}\})\\ &\times\sum_l{}'\exp(-i\mathbf{K}\,\mathbf{r}_l) + \frac{1}{2}\sum_{nn'l}{}'q_nq_{n'}\frac{\mathrm{erfc}(\eta r_{nn'l})}{r_{nn'l}},\end{aligned} \tag{A.6}$$

where n, n' label ions, and l defines the unit cell. Σ' implies that summations are excluded for the case $n = n'$, $l = 0$.

This equation may be simplified as follows. The sum $\Sigma_l\exp(-i\mathbf{K}.\mathbf{r}_l)$ is zero if the sum over lattice vectors is complete and vector **K** is other than 2π times a reciprocal lattice vector. When **K** is 2π times a reciprocal lattice vector, which we distinguish by the symbol **G**, then the sum over a complete set of lattice sites is N, the number of unit cells in the crystal.

Before exploiting this result, we must complete the sums to include a representation of the shell model. There is no self-interaction of a charge with itself and no Coulomb interaction between the core and shell of the same ion. Thus to complete the sums $\Sigma_l\exp(-i\mathbf{K}.\mathbf{r}_l)$, we add and then subtract explicitly the missing contributions which can be expressed directly as

$$\frac{2}{\pi^{1/2}}\int_0^{\eta}\exp(-r^2t^2)dt = \frac{\mathrm{erf}(\eta r)}{r}. \tag{A.7}$$

Therefore we write

$$\frac{1}{2}\sum_{nn'l}{}' \frac{q_n q_{n'}}{r_{nn'l}} = \left(\frac{1}{2}\right)\frac{4\pi}{v_c}\sum_{\mathbf{G}} \frac{\exp(-G^2/4\eta^2)}{G^2} \sum_{nn'} q_n q_{n'} \exp(-i\mathbf{G}.\{\mathbf{r}_n - \mathbf{r}_{n'}\}) - \frac{1}{2}\sum_{nn'}{}'' q_n q_{n'} \frac{\mathrm{erf}(\eta r_{nn'l})}{r_{nn'l}} + \frac{1}{2}\sum_{nn'l}{}' q_n q_{n'} \frac{\mathrm{erfc}(\eta r_{nn'l})}{r_{nn'l}}. \quad \text{(A.8)}$$

Here the sum $\Sigma''_{nn'}$ covers just those terms needed to complete the lattice sums $\Sigma_l \exp(-i\mathbf{K}.\mathbf{r}_l)$, that is the interaction of a core or shell with itself and the charge interaction of core and shell on the same ion. These, of course, are just the terms omitted in $\Sigma'_{nn'l}$ so it is convenient to amalgamate the sums by defining a function $H_{nn'l}(x)$ so that

$$H_{nn'l}(x) = \frac{\mathrm{erfc}(x)}{x}, \quad \text{(A.9a)}$$

except when $l = 0$ and either $n = n'$ or n and n' are the core and shell of the same ion. In this case

$$H_{nn'l}(x) = -\frac{\mathrm{erf}(x)}{x}. \quad \text{(A.9b)}$$

When $l = 0$ and $n = n'$, we actually need to calculate $H_{nn'l}(x)$ at $x = 0$ where the function is singular. However, $\mathrm{erf}(x)/x$ has a well-defined limit of $2/\pi^{1/2}$ as x tends to zero and we interpret the function in this sense.

We can further simplify the expression (A.8) for the Coulomb term in ways that aid subsequent discussion, in particular by evaluating real and imaginary parts of the phase factors. When we define

$$\begin{aligned} c_n(\mathbf{G}) &= q_n \cos(\mathbf{G}.\mathbf{r}_n) \\ s_n(\mathbf{G}) &= q_n \sin(\mathbf{G}.\mathbf{r}_n), \end{aligned} \quad \text{(A.10)}$$

we have

$$\sum_{nn'} q_n q_{n'} \exp(-i\mathbf{G}.\{\mathbf{r}_n - \mathbf{r}_{n'}\}) = \sum_{nn'} \{c_n(\mathbf{G}) - is_n(\mathbf{G})\}\{c_{n'}(\mathbf{G}) + is_{n'}(\mathbf{G})\} = \sum_{n} \{c_n(\mathbf{G}) - is_n(\mathbf{G})\} \sum_{n'} \{c_{n'}(\mathbf{G}) + is_{n'}(\mathbf{G})\} = C(\mathbf{G})^2 + S(\mathbf{G})^2, \quad \text{(A.11)}$$

where

$$\begin{aligned} C(\mathbf{G}) &= \sum_n c_n(\mathbf{G}) \\ S(\mathbf{G}) &= s_n(\mathbf{G}). \end{aligned} \quad \text{(A.12)}$$

For the convenience, we define an additional function

$$G(x) = \frac{\exp(-x)}{x}. \quad \text{(A.13)}$$

The expression (A.8) will then include a singular term $G(0)$, corresponding to the zero reciprocal lattice vector. However, in this case, the phases $\cos(\mathbf{G}.\mathbf{r}_n)$ and $\sin(\mathbf{G}.\mathbf{r}_n)$ are equal for all core and shell sites; thus, C(G) and S(G) are zero because the unit cell is neutral and $\Sigma_n q_n = 0$. Hence, we omit the zero reciprocal lattice vector in the sum Σ_G in Equation (A.8) and denote this explicitly as Σ'_G. Then, using Equations (A.9a), (A.9b), (A.11) and (A.13) to simplify (A.8), we find

$$\frac{1}{2}\sum_{nn'l}{}' \frac{q_n q_{n'}}{r_{nn'l}} = \left(\frac{1}{2}\right)\frac{\pi}{\eta^2 v_c}\sum_{\mathbf{G}}{}' G\left(\frac{G^2}{4\eta^2}\right)\{C(\mathbf{G})^2 + S(\mathbf{G})^2\} + \frac{1}{2}\sum_{nn'l}\eta H_{nn'l}(r_{nn'l}). \quad \text{(A.14)}$$

Finally, we define a general potential depending on the core or shell separations. Thus,

$$V_{nn'l}(r) = \phi_{nn'}(r) + \eta H_{nn'l}(\eta r), \quad \text{(A.15)}$$

where $\phi_{nn'}(r)$ is the short range potential acting between ions n and n', and clearly if $n = n'$ and $l = 0$ there is no explicit potential contribution $\phi_{nn'}(r)$. Since in calculating the lattice energy, this corresponds to $r_{nn'l} = 0$, we may simply require that $\phi_{nn'}(r)$ is zero when $r = 0$ and then the definition (A.15) requires no further qualification. Thus we have a final form for the unit cell energy;

$$U_c = \frac{1}{2}\frac{\pi}{\eta^2 v_c}\sum_{\mathbf{G}}{}' G\left(\frac{G^2}{4\eta^2}\right)\{C(\mathbf{G})^2 + S(\mathbf{G})^2\} + \frac{1}{2}\sum_{nn'l} V_{nn'l}(r_{nn'l}) \quad \text{(A.16)}$$

We base all subsequent discussion of the derivatives of the cell energy with respect to internal strains, that is the core and shell coordinates, and with respect to bulk strains on this form of the unit cell energy.

A complete discussion of formula (A.16) must consider the convergence of both the reciprocal and direct lattice sums. The direct lattice sum has explicit potential and Madelung parts. The potential usually has a fixed range but the Coulomb parts are more complex. In particular, the convergence of both the direct and reciprocal lattice sums depends on the choice of the parameter η.

If we consider, then, just the Madelung sums, as given by Equation (A.8), it is clear that both sums have terms of oscillating sign because of the charges and the phase factors $\exp(-i\mathbf{G}.\{\mathbf{r}_n - \mathbf{r}_{n'}\})$. Thus, it is very difficult to discuss the convergence of the series rigorously. However, because both the reciprocal and direct lattice sums converge very rapidly as $|\mathbf{G}|$ and $r_{nn'l}$ increase, we may determine the accuracy of the calculation by truncating the summations when the magnitudes of the next terms fall below a specified limit.

The series $\Sigma'_{nn'l}(q_n q_{n'})/r_{nn'l}$ is of dimension q^2/r and we may truncate the series when the excluded terms are smaller in magnitude than $A(q^2/r_0)$ where r_0 is a characteristic lattice length. The charges are all of the same magnitude and may be taken as order unity and r_0 is most conveniently chosen as $v_c^{1/2}$ where v_c is, of course, the volume of the unit cell.

Then, for the reciprocal lattice series, we define a parameter G_m and include in the sum all reciprocal lattice vectors with $|\mathbf{G}| < G_m$; in the same way we set a limit r_m and include terms in the direct lattice sums with $r_{nn'l} < r_m$. In order that these parameters should define limits to the series, from Equation (A.8) we require that

$$\frac{4\pi}{v_c}\frac{\exp(-G_m^2/4\eta^2)}{G_m^2} \leqslant \frac{A}{r_0} \quad \text{(A.17)}$$

and

$$\frac{\operatorname{erfc}(\eta r_m)}{r_m} \leqslant \frac{A}{r_0}. \quad \text{(A.18)}$$

Since we are concerned with evaluating the series to high accuracy, A is small and ηr_m is large enough to allow use of the first term in the asymptotic expansion for $\operatorname{erfc}(x)$. Thus Equation (A.18) may be replaced by

$$\frac{\text{erfc}(\eta r_m)}{r_m} \simeq \frac{\exp(-\eta^2 r_m^2)}{\eta r_m^2 \pi^{1/2}} \leqslant \frac{A}{r_0}. \tag{A.19}$$

We may conveniently find acceptable solutions to these inequalities by substituting the requirements that

$$\exp(-G_m^2/4\eta^2) = A \tag{A.20}$$

with

$$\frac{v_c G_m^2}{4\pi} \geqslant r_0 \tag{A.21}$$

and

$$\exp(-\eta^2 r_m^2) = A \tag{A.22}$$

with

$$\eta r_m^2 \pi^{1/2} \geqslant r_0. \tag{A.23}$$

The solutions for G_m and r_m from (A.20) and (A.22) are of course

$$G_m = 2\eta f \tag{A.24}$$

$$r_m = f/\eta \tag{A.25}$$

where

$$f = (-\ln A)^{1/2} \tag{A.26}$$

and in particular

$$G_m r_m = 2f^2. \tag{A.27}$$

We should now ensure the maximum efficiency of the method by an optimum choice of η. To this end we must consider the number of terms in each series for a particular choice of G_m and r_m. In the direct lattice, a value of r_m defines a volume of crystal $4\pi r_m^3/3$ that contains $4\pi r_m^3/3v_c$ unit cells and $4\pi r_m^3 s/3v_c$ lattice sites if s is the number of ions (actually cores + shells) per unit cell. Since we consider all pairs of interactions, the number of terms to be evaluated is thus $4\pi r_m^3 s^2/3v_c$.

In the reciprocal lattice, the volume defined by G_m is $4\pi G_m^3/3$ and since the volume per **G** vector is $8\pi^3/v_c$, the number of reciprocal lattice vectors is $v_c G_m^3/6\pi^2$. Although from Equation (A.8) it seems that there are s^2 terms, in fact from Equations (A.11) and (A.12) we see that the amount of calculation for each **G** vector depends only on s.

If we make the rough assumption that each term requires equal computation, then the necessary calculation depends on the total number of terms in both series, N_t, and

$$N_t = \frac{4\pi}{3}\left(\frac{r_m^3 s^2}{v_c} + \frac{G_m^3 v_c s}{8\pi^3}\right). \tag{A.28}$$

If we now substitute for r_m and G_m in terms of η using Equations (A.24) and (A.25), we have

$$N_t = \frac{4\pi f^3}{3}\left(\frac{s^2}{v_c \eta^3} + \frac{v_c s \eta^3}{\pi^3}\right). \tag{A.29}$$

Then the optimum value of the parameter η is chosen to satisfy $dN_t/d\eta = 0$; hence

$$\eta = \left(\frac{s\pi^3}{v_c^2}\right)^{1/6} \tag{A.30}$$

and with $r_0 = v_c^{1/3}$

$$\eta = s^{1/6}\pi^{1/2}/r_0. \tag{A.31}$$

Substituting in Equation (A.24) gives

$$G_m = 2s^{1/6}\pi^{1/2}f/r_0 \tag{A.32}$$

and in (A.25)

$$r_m = r_0 f/s^{1/6}\pi^{1/2}, \tag{A.33}$$

which are the optimum parameters to ensure most efficient calculation of the Madelung sums. However, we must check finally that these results satisfy the subsidiary inequalities (A.21) and (A.23).

If we substitute for G_m in (A.21), using Equation (A.32), we have

$$\frac{v_c G_m^2}{4\pi} = s^{1/3}f^2 r_0 \tag{A.34}$$

which exceeds r_0 if $s^{1/3}f^2 \geqslant 1$. We substitute (A.31) and (A.33) in (A.23) and find

$$\eta r_m^2 \pi^{1/2} = \frac{r_0 f^2}{s^{1/6}} \tag{A.35}$$

which exceeds r_0 if $f^2/s^{1/6} \geqslant 1$. This is the stronger of the two conditions since $s \geqslant 1$ (s is the number of cores and shells in the unit cell) but is satisfied for all realistic calculations. For example, with $A = 10^{-2}$, a very low accuracy, $f^2 = 4.6$ which admits values $s \lesssim 9500$. At higher accuracy, the restrictions on s become even less severe. Thus, we find the subsidiary inequalities to Equations (A.20) and (A.22) are satisfied for all realistic circumstances.

References

[1] D. Olson and A. Bisio, eds, *Proceedings of the Sixth International Zeolite Conference*, Butterworths, Guildford, 1984.

[2] J.V. Smith, "Enumeration of 4-connected 3 dimensional nets and classification of framework silicates, III", *Am. Miner.*, **64**, 551 (1979).

[3] R. Fletcher and M.J.D. Powell, "A rapidly convergent descent method for minimisation", *Comput. J.* **6**, 163 (1963).

[4] A.T.J. Hope, "Experimental and theoretical studies on pentasil zeolites", *PhD thesis*, University of London, UK, 1985.

[5] S.C. Parker, "Computer modelling of minerals", *PhD thesis*, University of London, UK, 1983.

[6] S.C. Parker, private communication.

[7] C.R.A. Catlow and W.C. Mackrodt, eds, *Computer Simulations of Solids*, Lecture Notes in Physics No. 166, Springer-Verlag, Berlin, 1982.

[8] B.G. Dick and A.W. Overhauser, "Theory of the dielectric constants of alkali halide crystals", *Phys. Rev.*, **112**, 90 (1958).

[9] R.G. Gordon and Y.S. Kim, "Theory for the forces between closed-shell atoms and molecules", *J. Chem. Phys.*, **56**, 3122 (1972).

[10] M.J. Sanders and C.R.A. Catlow, "The cation distribution in faujasites", in *Proceedings of the Sixth International Zeolite Conference*, D. Olson, A. Bisio, eds., Butterworths, Guildford, 1984, ch. 12.

[11] M.J. Sanders, "Computer simulation of framework structured minerals", *PhD thesis*, University of London, UK, 1984.
[12] W.J. Mortier, H.J. Bosmans and J.B. Uytterhoeven, "Location of univalent cations in synthetic zeolites of the Y and X type with varying silicon to aluminium ratio. II. Dehydrated potassium exchanged forms", *J. Phys. Chem.*, **76**, 650 (1972).
[13] M.J. Sanders, C.R.A. Catlow and J.V. Smith, "Crystal energy calculations for strontium ions in zeolite A", *J. Phys. Chem.*, **88**, 2796 (1984).
[14] R.L. Firor and K. Seff, "Near zero coordinate Ca^{2+} and Sr^{2+} in zeolite A. Crystal structures of dehydrated Ca_6-A and Sr_6-A", *J. Am. Chem. Soc.*, **100**, 3091 (1978).
[15] J.J. Pluth and J.V. Smith, "Crystal structure of dehydrated Sr-exchanged zeolite A. Absence of near-zero-coordinate Sr^{2+}. Presence of Al complex", *J. Am. Chem. Soc.*, **104**, 6977 (1982).
[16] J.J. Pluth and J.V. Smith, "Accurate redetermination of crystal structure of dehydrated zeolite A. Absence of near zero coordination of sodium. Refinement of Si, Al-ordered superstructure", *J. Am. Chem. Soc.*, **102**, 4704 (1980).
[17] D.H. Olson, G.T. Kokotailo, S.L. Lawton and W.M. Meier, "Crystal structure and structure-related properties of ZSM-5", *J. Phys. Chem.*, **85**, 2238 (1981).
[18] C.R.A. Catlow and M.J. Norgett, "Lattice structure and stability of ionic materials", *UKEA Report AERE-M2936* (1976).
[19] M.P. Tosi, "Cohesion of ionic solids in the Born model", *Solid State Physics*, **16**, 1 (1964).